79-0-0508

NTIS, AD-A063 792/6GA

AGARD

ADVISORY GROUP FOR AEROSPACE RESEARCH & DEVELOPMENT

7 RUE ANCELLE 92200 NEUILLY SUR SEINE FRANCE

Paper Reprinted from

Conference Proceedings No. 238

OPERATIONAL MODELLING OF THE AEROSPACE PROPAGATION ENVIRONMENT

NORTH ATLANTIC TREATY ORGANIZATION

AEROSPACE PROPAGATION PREDICTION CAPABILITIES ASSOCIATED WITH THE IF-77 MODEL

M. E. Johnson and G. D. Gierhart
Office of Telecommunications
Institute for Telecommunication Sciences
Boulder, Colorado 80303, U.S.A.

SUMMARY

The United States Department of Commerce (DOC) has been active in radio wave propagation research and prediction for several decades, and has provided the Federal Aviation Administration (FAA) with many propagation predictions relevant to the coverage of air navigation and communications systems. During 1960-1973, an air/ground propagation model applicable to irregular terrain was developed by the Office of Telecommunications/ Institute for Telecommunication Sciences (OT/ITS) for the FAA and was documented in detail. This IF-73 (ITS-FAA-1973) propagation model has evolved into the IF-77 model, which is applicable to air/ground, air/air, ground/satellite, and air/satellite paths. It can also be used for ground/ground paths that are line-of-sight, smooth earth, or have a common horizon. Model applications are restricted to telecommunication links operating at radio frequencies from about 0.1 to 20 GHz with antenna heights greater than 0.5 m. In addition, the elevation of the radio horizon must be less than the elevation of the higher antenna. The radio horizon for the higher antenna is taken either as a common horizon with the lower antenna or as a smooth earth horizon with the same elevation as the lower antenna's effective reflecting plane.

This propagation model has been incorporated into ten computer programs. These programs may be used to obtain a wide variety of computer-generated microfilm plots such as transmission loss versus path length and desired-to-undesired signal ratio at a receiving location versus the distance separating the desired and undesired transmitting facilities. Such capabilities are useful in estimating the service coverage of aerospace radio systems, and are currently being used to establish station separation requirements for VHF/UHF/SHF air navigation aids. This paper provides (1) a brief discussion of the IF-77 propagation model, (2) a summary of the prediction capabilities available, and (3) remarks concerning model validation work.

1. INTRODUCTION

Assignments for aeronautical radio in the radio frequency spectrum must be made so as to provide reliable services for an increasing air traffic density. Potential interference between facilities operating on the same or on adjacent channels must be considered in expanding present services to meet future demands. Service quality depends on many factors including the desired-to-undesired signal ratio at the receiver. This ratio varies with receiver location and time even when other parameters, such as antenna gain and radiated powers, are fixed.

The prediction capabilities mentioned in this paper were developed at OT/ITS with the sponsorship of the FAA. Although these were intended for use in predicting the service coverage associated with ground- or satellite-based VHF/UHF/SHF air navigation aids, they can be used for other services.

2. PROPAGATION MODEL

At 0.1 to 20 GHz, propagation of radio energy is affected by the lower nonionized atmosphere (troposphere), specifically by variations in the refractive index of the atmosphere. Atmospheric absorption and attenuation or scattering due to rain become important at SHF. The terrain, along and in the vicinity of the great circle path between transmitter and receiver also plays an important part. In this frequency range, time and space, variations of received signals, and interference ratios lend themselves readily to statistical description.

Conceptually, the model is very similar to the Longley-Rice propagation model for propagation over irregular terrain, particularly in that attenuation versus distance curves calculated for the (a) line-of-sight, (b) diffraction, and (c) scatter regions are blended together to obtain values in transition regions (Longley and Rice, 1968). In addition, the Longley-Rice relationships involving the terrain parameter Δh are used to estimate radio horizon parameters when such information is not available from facility siting data. The model includes allowance for

(a) average ray bending (Bean and Dutton, 1968; sec. 3),

(b) horizon effects (Gierhart and Johnson, 1973, sec. A.4.1),

(c) long-term power fading (Rice et al., 1967, sec. 10),

(d) vertical plane patterns for both antennas (Hartman, 1974, sec. CI-D.3),

(e) surface reflection multipath (Hartman, 1974, sec. CI-D.7),

(f) tropospheric multipath (Gierhart and Johnson, 1973, sec. A.7),

(g) atmospheric absorption (Rice et al., 1967, sec. 3),

(h) ionospheric scintillations (Whitney et al., 1971),

(i) rain attenuation (Samson, 1975, sec. 3),

(j) reflection from an elevated counterpoise (Gierhart and Johnson, 1973, sec. A.4.2),

(k) smooth earth diffraction (Longley and Rice, 1968, sec. 3.2),

(l) knife-edge diffraction (Longley and Reasoner, 1970, sec. 3.5), and

(m) forward scatter (Rice et al., 1967, sec. 9).

Input parameters for IF-77 are summarized in figure 1. Note that the minimum parameter requirement is frequency and antenna elevations (H1 and H2).

The above discussion provides a very brief description of the IF-77 model and contains sufficient specific references to allow readers to pursue topics of interest to them. However, additional discussion is provided here for some parts of the model that may be of particular interest in connection with the predictions made for aerospace systems with line-of-sight service limitations; i.e., power available (sec. 21.), median basic transmission loss (sec. 2.2), and variability (sec. 2.3).

2.1. Power Available

Power available as calculated in IF-77 is taken as the power available from the receiving antenna terminals under matched conditions when internal heat losses of the receiving antenna and path antenna gain loss are neglected. Compensation for internal heat loss or gain-loss factors needed to refer the available power to some point in the receiving system other than the receiving antenna terminals can be made by an appropriate adjustment to the radiated power or antenna gains used for computer program input.

Power available $P_a(q)$ levels exceeded for a fraction of time q are determined using

$$P_a(q) = \text{EIRPG} + G_{NT} + G_{NR} - L_b(0.5) + Y_\Sigma(q) \text{ dBW,} \quad (1)$$

$$\text{EIRPG} = \text{EIRP} + G_R \text{ dBW,} \qquad \text{and} \quad (2)$$

$$\text{EIRP} = P_{TR} + G_T \text{ dBW.} \quad (3)$$

Here EIRP is equivalent isotropically radiated power, P_{TR} in decibels greater than 1 W (dBW) is the total power radiated by the transmitting antenna, and $G_{T,R}$ in decibels greater than isotropic (dBi) is the maximum gain of the transmitting antenna or receiving antenna respectively. Losses (e.g., lines) associated with the transmitting system should be considered in calculating radiated power from transmitter output power. Normalized antenna gain (G_{NT} or G_{NR}) in decibels greater than maximum gain (G_T or G_R) is included in (1) to allow for antenna directivity when maximum gain is not appropriate (i.e., the antennas are not pointed at each other). A tracking option is available that keeps antenna main beams pointed at each other. Methods used to calculate the median basic transmission loss, L_b (0.5), and the total variability with time, $Y_\Sigma(q)$, are discussed in section 2.2 and 2.3. Note that $Y_\Sigma(q)$ is the only term on the right-hand side of (1) that contains variability with time when path parameters (e.g., distance, heights, etc.) are fixed, and EIRP is considered to be constant with time.

2.2. Median Basic Transmission Loss

Median basic transmission loss $L_b(0.5)$ is calculated from

$$L_b(0.5) = L_{bf} + A_a + A_{cr} - V_e(0.5) \text{ dB,} \quad (4)$$

where L_{bf} is basic transmission loss for free space, A_a is average atmospheric absorption, A_{cr} is a reference attenuation calculated for the propagation mode(s) applicable for a particular path (e.g., line-of-sight variability, line-of-sight lobing, diffraction, scatter, or transition regions), and $V_e(0.5)$ is a median adjustment associated with long-term variability.

With the variability option, lobing associated with a specular reflection from the earth's surface is suppressed inside the far portion of the horizon lobe. When lobing is suppressed in this way, an appropriate increase in the variability associated with short-term variability (sec. 2.3) is made. A conditional adjustment factor, A_Y, that is a function of the long-term variability is used to prevent available power levels from exceeding levels expected for free-space propagation by an unrealistic amount when the long-term variability about $L_b(0.5)$ is large; i.e., A_{cr} is increased so that the long-term power does not exceed its free-space value by 3 dB for more than 10 percent of the time. Lobing associated with a counterpoise reflection is included in A_{cr} even when the variability option is used.

With the lobing option, lobing associated with interference between the direct ray and specular reflections from both the counterpoise and the earth's surface are allowed to determine A_{cr} for the first 10 lobes inside the smooth earth radio horizon. Contributions to short-term variability associated with the specular earth's surface reflection are neglected when A_{cr} is based on lobing. The program calculates several points for each of the 10 lobes inside the horizon. One of these will be the lobe null if no counterpoise reflected ray is present and the phase change associated with reflection is 180°. Otherwise, calculations may not actually be made for the null case. Conditions most likely to result in missed nulls involve the propagation of vertical polarization over sea water or transition regions where both the earth surface and counterpoise reflected rays are significant.

Calculation of A_{cr} in the diffraction region involves a weighted average of rounded earth and knife-edge diffraction attenuations. Transition between the line-of-sight and diffraction regions is made using a straight line connecting a diffraction value at the radio horizon with a point in the line-of-sight region where the ray optics formulation is valid.

2.3. Variability

The variability term of (1) is calculated from

$$Y_\Sigma(q) = \pm\sqrt{Y_e^2(q) + Y_\pi^2(q) + Y_r^2(q) + Y_I^2(q)} \quad \text{dB}, \tag{5}$$

$$+ \text{ for } q \le 0.5$$

$$- \text{ otherwise}$$

where $Y_e(q)$ is long-term (hourly-median) variability, $Y_\pi(q)$ is variability associated with surface reflection and tropospheric multipath, $Y_r(q)$ is rain attenuation variability, and $Y_I(q)$ is variability associated with ionospheric scintillation. The short-term (within the hour) variabilities $Y_\pi(q)$, $Y_r(q)$, and Y_I are neglected if the option for long-term variability only is selected; i.e., $Y_\Sigma(q) = Y_e(q)$ when the option to predict the distribution of hourly median levels is selected. The median level of $P_a(q)$ is not dependent on $Y_\Sigma(q)$ since $Y_\Sigma(0.5) = Y_e(0.5) = Y_\pi(0.5) = Y_r(0.5) = 0$.

The IF-77 model contains long-term variability options which allow variabilities for different climates or time blocks within a continental temperate climate to be selected. These variabilities are similar to, but not identical with, those provided by Technical Note 101 (Rice et al., 1967), or the CCIR, (1970). Techniques used in IF-73 to prevent excessive long-term variability are still used.

Nakagami-Rice distributions are used for $Y_\pi(q)$ (Rice et al., 1967, p. V-8). These distributions provide statistics for the case where a constant vector is added to a Rayleigh-distributed vector. The particular distribution applicable is selected by a parameter K where K is the ratio in decibels between the steady component of received power and the Rayleigh fading component. If K is large (> 40 dB), $Y_\pi(q) = 0$, and if K is small (< -20 dB), $Y_\pi(q)$ is a Rayleigh distribution. Power for the Rayleigh distributed vector is taken as the sum of relative powers associated with surface reflection multipath and tropospheric multipath.

Surface reflection multipath is calculated from effective reflection coefficients for specular and diffuse reflection from the earth's surface. When the specular component is used to produce lobing (i.e., lobing option selected), it is neglected in the calculation of surface reflection multipath power. These effective reflection coefficients include allowances for surface constants, frequency, surface roughness, relative direct-reflected ray antenna gain, relative direct-reflected ray lengths, counterpoise shadowing, and divergence. Counterpoise reflection is always allowed to cause lobing and is never allowed to contribute to $Y_\pi(q)$. For beyond-the-horizon paths, surface reflection multipath contributions are neglected.

The tropospheric multipath power formulation for the line-of-sight region was derived from an outage time formulation developed for microwave relay links (Lenkurt, 1970, pp. 60, 13-2, 119). Just beyond the horizon, the formulation involves a linear interpolation between the K parameter value applicable at the radio horizon and a K = -20 dB value used in the scatter region. Data (Janes, 1955) were used to determine the distance beyond which short-term fading for beyond-the-horizon paths can be characterized as Rayleigh (K ≤ -20 dB).

Rain attenuation variability is based on an extension of work done by Samson, (1975, sec. 3). The formulation involves

$$Y_r(q) = \begin{Bmatrix} 0 \text{ for } q \le 0.98 \\ A_{rr}(q)\, r_s \text{ otherwise} \end{Bmatrix} \quad \text{dB} \tag{6}$$

where $A_{rr}(q)$ is the rain attenuation rate determined using rain rate statistics, and r_s is an in-storm ray length. Note that $Y_r(q) = 0$ for time availabilities less that 98%.

Ionospheric scintillation variability is described with the distributions given by Whitney et al., (1971). The model does not predict the ionospheric scintillation index; i.e., an appropriate value is selected for an ionospheric scintillation group number which is a model input parameter.

3. PROGRAMMED CAPABILITIES

The IF-77 model has been incorporated into ten computer programs which provide 28 plotting capabilities. These programs cause the computer to produce parameter summary sheets and microfilm plots. A guide to the plotting capabilities currently available is provided in figure 2, and a sample parameter sheet is shown in figure 3. An applications guide covering these programs is being prepared (Johnson and Gierhart, 1978).

Capabilities 1 through 10 are outputs from a single program called LOBING (Hartman, 1974, sec. CII). This program uses an abbreviated version of IF-77 that is applicable only to the line-of-sight region for a spherical earth in which variability with time and horizon effects are neglected. Various parameters such as transmission loss, reflection coefficient, time lag, and elevation angle are plotted against path distance. Figure 4 is a transmission loss curve in which the lobing caused by interference between direct and reflected ray is shown along with limiting and free space values. Flight through such a lobing structure will cause periodic variation in received level, and the lobe or doppler-beat modulation frequency (Reed and Russell, 1964, sec. 10) associated with it can be estimated using the lobing frequency plots of capabilities 5 and 6. These plots are normalized with respect to carrier frequency, and aircraft velocity such that the radial component of velocity is used with capability 5 and the vertical component is used with capability 6 (Hartman, 1974, secs. CII-C.6, CII-C.7).

Capabilities 11 through 23 provide information relevant to received signal level as power available, power density, transmission loss, or the equivalent isotropically radiated power needed to obtain a specified power density. The selected quantity may be used as the ordinate for capabilities 11 through 16, or shown as contours for specific levels in the altitude versus distance plane for capabilities 17 through 23.

Figure 5 was produced by using capability 13 for parameters of figure 3 which are identical to those used for figure 4 except that the option to include lobing as part of the time variability was used along with the nautical mile plotting option. Figure 5 shows the transmission loss predicted under free space conditions along with loss levels expected to be unexceeded during 5, 50, and 95 percent of the time. In addition, the lobing pattern from figure 4 has been superimposed to illustrate the difference between the two ways of treating lobing. Note that the 95 percent loss is not as great as the loss encountered in a null, but that it is usually greater than the loss predicted by the lobing model. The monotonic nature of the curves developed with the variability option make them more convenient to use in service range predictions. However, if the frequency and antenna heights are such that only a few lobes are present, the lobing option is probably preferable since it provides information on the location of strong and weak signal regions. These regions are both large and stable in that changes of refractive conditions or uncertainty associated with the precise aircraft location would not drastically alter the received signal level.

Capabilities 24 through 28 provide information on the desired to undesired signal ratio, D/U, available at the aircraft when transmissions from two facilities are received simultaneously. The interference configuration is illustrated in figure 6. Note that station separation, S, is defined as the sum of d_D and d_U so that S is equal to the great-circle facility separation, S_f, only when the facilities and the aircraft are along the same great circle.

Capabilities 24 and 25 provide curves of D/U versus S or d_D, respectively. Figure 7 was developed using capability 24. It can be used to estimate the station separation needed to obtain a required D/U value for the specified aircraft location (altitude and d_D).

Figure 8 was developed using capability 26. Curves showing the relative azimuthal orientation of the undesired facility, ϕ_U, with respect to the great-circle path connecting the desired and undesired facility are plotted versus the facility separation required to achieve a required D/U ratio or better at each of six specified protection points. Each curve represents a different relative azimuthal orientation of the desired facility, ϕ_D, with respect to the path connecting facilities.

Orientation geometry for the protection points is illustrated in figure 9. Protection point C is used to illustrate the difference between facility separation, S_f, used in figure 8, and station separation, S, used elsewhere (fig. 7). In particular, $S_f \leq S$ since S need not be measured along the great-circle path connecting the facilities. Note that (a) the d_U to point C changes as ϕ_D changes even if S_f remains fixed, and (b) the angle from the undesired facility to point C changes with both ϕ_D and ϕ_U, so that the applicable gain for the undesired facility varies in accordance with its horizontal pattern even if S_f remains fixed.

The geometrical consequences of these complications are handled as part of the calculations performed by program TWIRL. These calculations would be very tedious to perform by hand even if appropriate signal ratio graphs (fig. 9) were available. A graph similar to figure 8 is constructed for each protection point, and the maximum S_f for each combination of ϕ_D and ϕ_U is selected for the final graph (fig. 8). These intermediate graphs have a format identical to figure 8 and are available as computer output even though no samples are provided here.

Capabilities 27 and 28 provide contours for fixed D/U values in the altitude versus distance plane for a fixed facility separation. With capability 27, a single D/U value is used with 3 different time availabilities, whereas capability 28 involves a fixed time availability and several D/U values. Figure 10 was produced using capability 28.

4. MODEL VALIDATION

Model validation work is being done by comparing predictions made using IF-77 with measured data and other predictions. While this work will eventually involve comparisons with data from many sources, the remarks made here involve only those data obtained from a single data source (Longley et al., 1971). This source was selected for our initial effort because it (a) "...summarizes measurements of tropospheric transmission loss and its long-term variability for nearly 800 paths in various parts of the world"; (b) contains sufficient information on path parameters, including path profiles, for IF-77 input; and (c) provides predictions based on two other widely used models.

Figure 11 is a sample of the comparisons being made. It is a copy of a figure from the data source to which a prediction made with IF-77 (labeled FAA) has been added. The other predictions were made with the Technical Note 101 method (Rice et al., 1967), and the ESSA 70 Model (Longley and Reasoner, 1970).

About 200 paths in the data source can be predicted using IF-77, and figures similar to figure 11 are being developed for them. Then statistics for the difference between predicted and measured median transmission loss values will be determined as a function of path type for each of the three models mentioned here.

5. REFERENCES

Bean, B. R., and E. J. Dutton, 1968, Radio Meteorology (Dover Publications, Inc., New York, N. Y.).

CCIR, 1970, Estimation of tropospheric-wave transmission loss, Report 244-2 XII Plenary Assembly, New Delhi, Vol. II, Part I (Intl. Telecomm. Union, Geneva).

Gierhart, G. D., and M. E. Johnson, 1973, Computer programs for air/ground propagation and interference analysis, 0.1 to 20 GHz, DOT Rept. FAA-RD-73-103 (NTIS, AD 770 335).

Hartman, W. J., editor, 1974, Multipath in air traffic control frequency bands, DOT Rept. FAA-RD-74-75, I and II, (NTIS, AD/A 006 267, and AD/A 006 268).

Janes, H. B., 1955, An analysis of within-the-hour fading in the 100-to-1000 Mc transmission, J. Res. NBS 54, No. 4, 231-250.

Johnson, M. E., and G. D. Gierhart, 1978, Applications guide for propagation and interference analysis computer programs (0.1 to 20 GHz), DOT Rept. FAA-RD-77-60 (to be printed).

Lenkurt, 1970, Engineering considerations for Microwave Communication Systems (GTE Lenkurt Dept., C134, San Carlos, Calif., $10.00).

Longley, A. G., and R. K. Reasoner, 1970, Comparison of propagation measurements with predicted values in the 20 to 10,000 MHz range, ESSA Tech. Rept. 148-ITS 97 (NTIS, AD 703 579).

Longley, A. G., R. K. Reasoner, and V. L. Fuller, 1971, Measured and predicted long-term distributions of tropospheric transmission loss, OT Rept. OT/TRER 16 (NTIS, COM 75-11205).

Longley, A. G., and P. L. Rice, 1968, Prediction of tropospheric radio transmission loss over irregular terrain, a computer method--1968, ESSA Tech. Rept., ERL 79-ITS 67 (NTIS, AD 676 874).

Reed, H. R., and C. M. Russell, 1964, Ultra High Frequency Propagation (Boston Tech. Publishers, Lexington, Mass.)

Rice, P. L., A. G. Longley, K. A. Norton, and A. P. Barsis, 1967, Transmission loss predictions for tropospheric communication circuits, NBS Tech. Note 101, I and II revised (NTIS, AD 687 820, and AD 687 821).

Samson, C. A., 1975, Atmospheric considerations in radio systems engineering at 10 to 30 GHz, OT Rept. 75-66 (NTIS, COM-75-11095/AS).

Whitney, H. E., J. Aarons, and D. R. Seemann, 1971, Estimation of the cumulative amplitude probability distribution function of ionospheric scintillations, AF Cambridge Res. Labs. Rept. AFCRL-71-0525, Cambridge, Mass.

PARAMETER	RANGE
Aircraft (or higher) antenna height above mean sea level (msl), H1	≥ Facility horizon height
Facility (or lower) antenna height above facility site surface (fss), H2	> 1.5 ft (0.5 m) above fss
Frequency	0.1 to 20 GHz
Specification of the following parameters is optional	
Aircraft antenna type options	Isotropic,* or as specified*
Polarization options	None, identical with facility
Tracking options	Directional* or tracking
Effective reflection surface elevation above msl	At fss* or specified value above msl
Equivalent isotropically radiated power	0.0 dBW* or specified
Facility antenna type options	Isotropic* or as specified
Counterpoise diameter	0* to 500 ft (152 m)
Height above fss	0* to 500 ft (152 m) Below facility antenna by at least 3 ft (1 m) but no more than 2000 ft (610 m)
Polarization options	Horizontal,* vertical, or circular
Tracking	Directional* or tracking
Gain, receiving antenna (main beam)	0* to 60 dBi
Transmitting antenna (main beam)	0* to 60 dBi
Transmitting antenna location	Aircraft or facility*
Horizon obstacle distance from facility	From 0.1 to 3 times smooth earth horizon distance (calculated)*
Elevation angle above horizontal at facility	<12 deg (calculated)*
Height above msl	0* to 15,000 ft-msl (4572 m-msl) and ≤ aircraft altitude
Ionospheric scintillation options	No scintillation* or specified
Index group	0* to 5, 6 for variable
Rain attenuation options	None* or computed with dB/km or zone
Attenuation/km	0 dB/km and up
Storm size	5, 10,* 20 km
Zone	1 to 6
Refractivity	
Effective earth's radius	4010 to 6070 n mi (7427 to 11,242 km)
or minimum monthly mean, N_o	200 to 400 N-units (301 N-units)*
Surface reflection lobing options	Contributes to variability* or determines median level
Surface type options	Poor, average* or good ground, fresh or sea water, concrete, metal
Sea state	0-glassy,* 1-rippled, 2-smooth, 3-slight, 4-moderate, 5-rough, 6-very rough, 7-high, 8-very high, 9-phenomenal
or rms wave height, σ_h	0 to 50 m (164 ft)
Temperature	0, 10,* or 20°C
Terrain elevation above msl at facility	0* to 15,000 ft-msl (4572 m-msl)
Parameter, Δh	0* or greater
Time availability options	For instantaneous levels exceeded* or for hourly median levels exceeded
Climates	0*-Continental all year, 1-Equatorial, 2-Continental subtropical, 3-Maritime subtropical, 4-Desert, 6-Continental Temperate, 7a-Maritime Temperate Overland, 7b-Maritime Temperate Overseas
or time blocks	1, through 8, summer, winter

*Values or options that will be assumed when specific designations are not made are flagged by asterisks.

Figure 1. Input parameters for IF-77.

CAPABILITY	REMARKS*
1. LOBING**	Transmission loss versus path distance.
2. REFLECTION COEFFICIENT**	Effective specular reflection coefficient versus path distance.
3. PATH LENGTH DIFFERENCE**	Difference in direct and reflected ray lengths versus path distance.
4. TIME LAG**	Same as above but with path length difference expressed as time delay.
5. LOBING FREQUENCY-D**	Normalized distance lobing frequency versus path distance.
6. LOBING FREQUENCY-H**	Normalized height lobing frequency versus path distance.
7. REFLECTION POINT**	Distance to reflection point versus path distance.
8. ELEVATION ANGLE**	Direct ray elevation angle versus path distance.
9. ELEVATION ANGLE DIFFERENCE**	Angle by which the direct ray exceeds the reflected ray versus path distance.
10. SPECTRAL PLOT**	Amplitude versus frequency response curves at various path distances.
11. POWER AVAILABLE	Power available at receiving antenna versus path distance or central angle for time availabilities of 5, 50 and 95%, and fixed antenna heights.
12. POWER DENSITY	Similar to above, but with power density ordinate.
13. TRANSMISSION LOSS	Similar to above, but with transmission loss ordinate.
14. POWER AVAILABLE CURVES	Power available curves versus distance are provided for several aircraft altitudes for a selected time availability, and a fixed lower antenna height.
15. POWER DENSITY CURVES	Similar to above, but with power density as ordinate.
16. TRANSMISSION LOSS CURVES	Similar to above, but with transmission loss as ordinate.
17. POWER AVAILABLE VOLUME	Fixed power available contours in the altitude versus distance plane for time availabilities of 5, 50, and 95%.
18. POWER DENSITY VOLUME	Similar to above, but with fixed power density contours.
19. TRANSMISSION LOSS VOLUME	Similar to above, but with fixed transmission loss contours.
20. EIRP CONTOURS	Contours for several EIRP levels needed to meet a particular power density requirement are shown in the altitude versus distance plane for a single time availability.
21. POWER AVAILABLE CONTOURS	Similar to above, but with power available contours for a single EIRP.
22. POWER DENSITY CONTOURS	Similar to above, but with power density contours.
23. TRANSMISSION LOSS CONTOURS	Similar to above, but with transmission loss contours.
24. SIGNAL RATIO-S	Desired-to-undesired, D/U, signal ratio versus station separation for a fixed desired facility-to-aircraft distance, and time availabilities of 5, 50, and 95%.
25. SIGNAL RATIO-DD	Similar to above, but the abscissa is desired facility-to-aircraft distance and the station separation is fixed.
26. ORIENTATION	Undesired facility antenna orientation with respect to the desired-to-undesired station line versus required facility separation curves are plotted for several desired facility antenna orientations.
27. SERVICE VOLUME	Fixed D/U contours are shown in the altitude versus distance plane for a fixed station separation and time availabilities of 5, 50, and 95%.
28. SIGNAL RATIO CONTOURS	Contours for several D/U values are shown in the altitude versus distance plane for a fixed station separation, and time availability.

*Additional discussion, by capability, will be provided in an "Applications Guide", which should be published in 1978 (Johnson and Gierhart, 1978).

**Applicable only to the line-of-sight region for spherical earth geometry. Variability with time and horizon effects are neglected.

Figure 2. Plotting capability guide for IF-77 programs.

PARAMETERS FOR ITS PROPAGATION MODEL IF-77
77/07/13. 22.15.49 RUN

TRANSMISSION LOSS

SPECIFICATION REQUIRED

AIRCRAFT (OR HIGHER) ANTENNA ALTITUDE: 45000. FT (13716.M) ABOVE MSL
FACILITY (OR LOWER) ANTENNA HEIGHT: 50.0 FT (15.2M) ABOVE FSS
FREQUENCY: 125. MHZ

SPECIFICATION OPTIONAL

AIRCRAFT ANTENNA TYPE: ISOTROPIC
    POLARIZATION: HORIZONTAL
EFFECTIVE REFLECTION SURFACE ELEVATION ABOVE MSL: 0. FT (0.M)
EQUIVALENT ISOTROPICALLY RADIATED POWER: 14.0 DBW
FACILITY ANTENNA TYPE: ISOTROPIC
    POLARIZATION: HORIZONTAL
HORIZON OBSTACLE DISTANCE: 8.69 N MI (16.09KM) FROM FACILITY*
    ELEVATION ANGLE: -0/ 6/30 DEG/MIN/SEC ABOVE HORIZONTAL*
    HEIGHT: 0. FT (0.M) ABOVE MSL
REFRACTIVITY:
    EFFECTIVE EARTH RADIUS: 4586. N MI (8493.KM)*
    MINIMUM MONTHLY MEAN: 301. N-UNITS AT SEA LEVEL
SURFACE REFLECTION LOBING: CONTRIBUTES TO VARIABILITY
SURFACE TYPE: AVERAGE GROUND
TERRAIN ELEVATION AT SITE: 0. FT (0.M) ABOVE MSL
TERRAIN PARAMETER: 0. FT (0.M)
TIME AVAILABILITY: FOR INSTANTANEOUS LEVELS EXCEEDED

* COMPUTED VALUE

Notes: 1) Parameter values (or options) not indicated are taken as the assumed values (or options) provided on the general parameter specification sheet (fig. 1).

2) To simulate computer output, only upper case letters are used. Dual units are not provided on actual computer output.

Figure 3. Parameter sheet for capability 13.

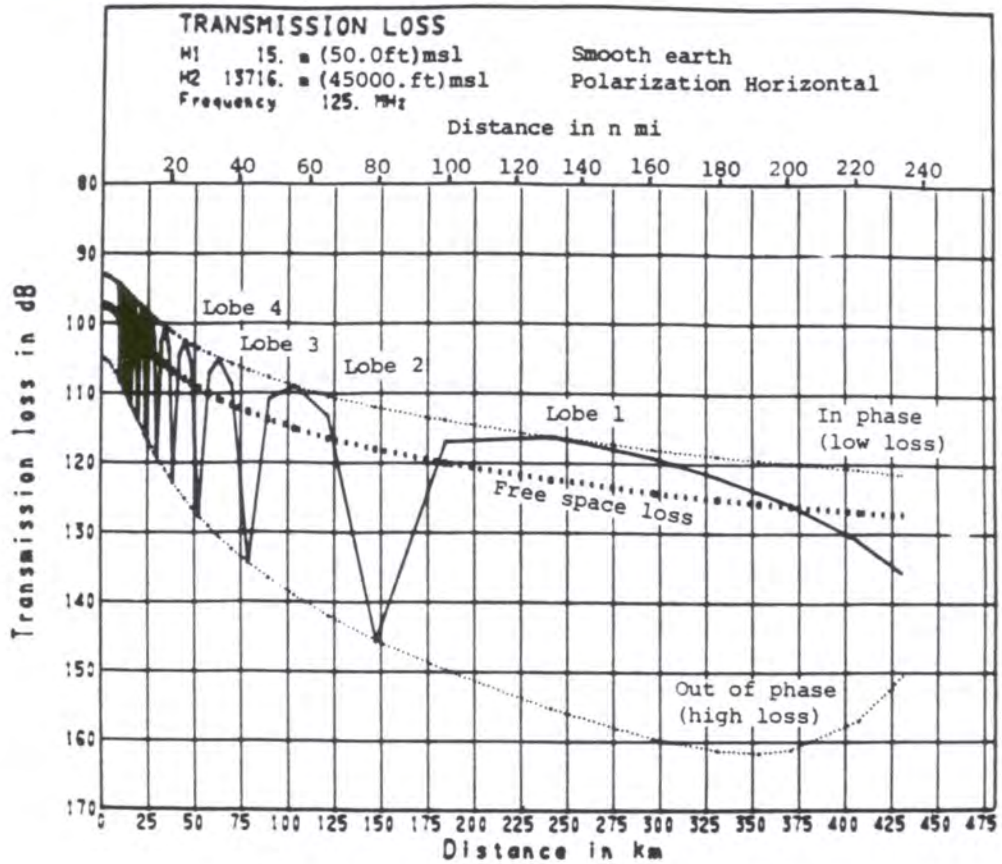

Figure 4. Plot for capability 1, LOBING.

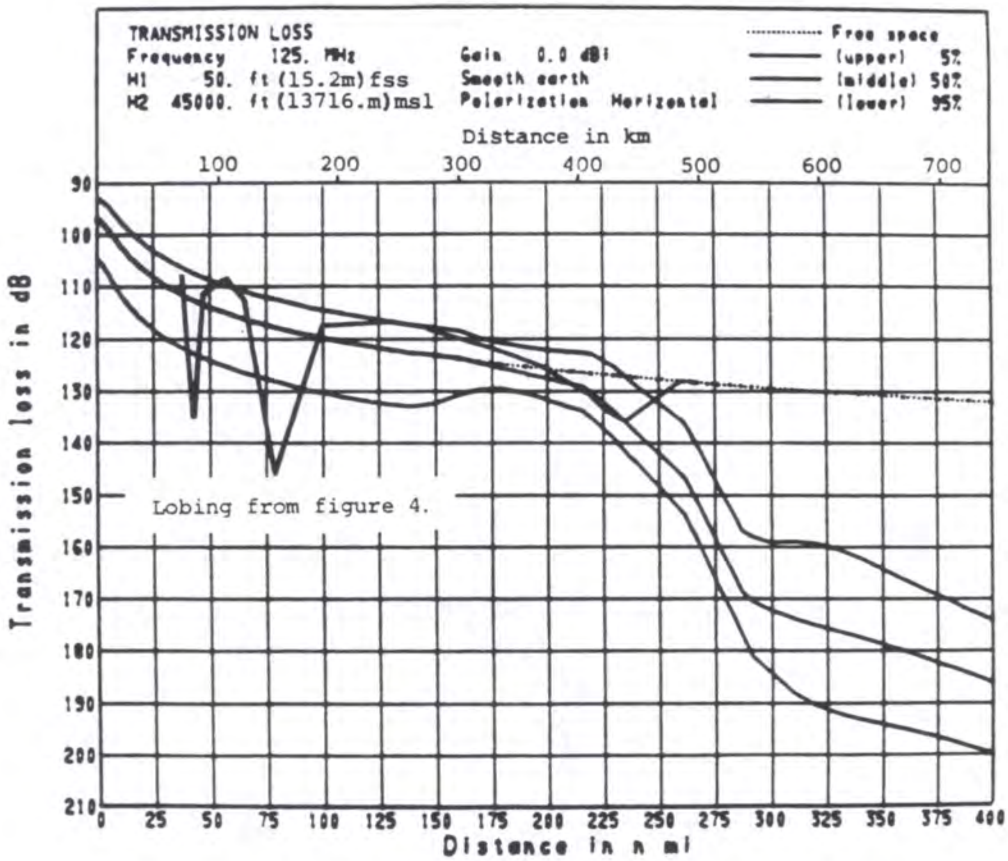

Figure 5. Plot for capability 13, TRANSMISSION LOSS.

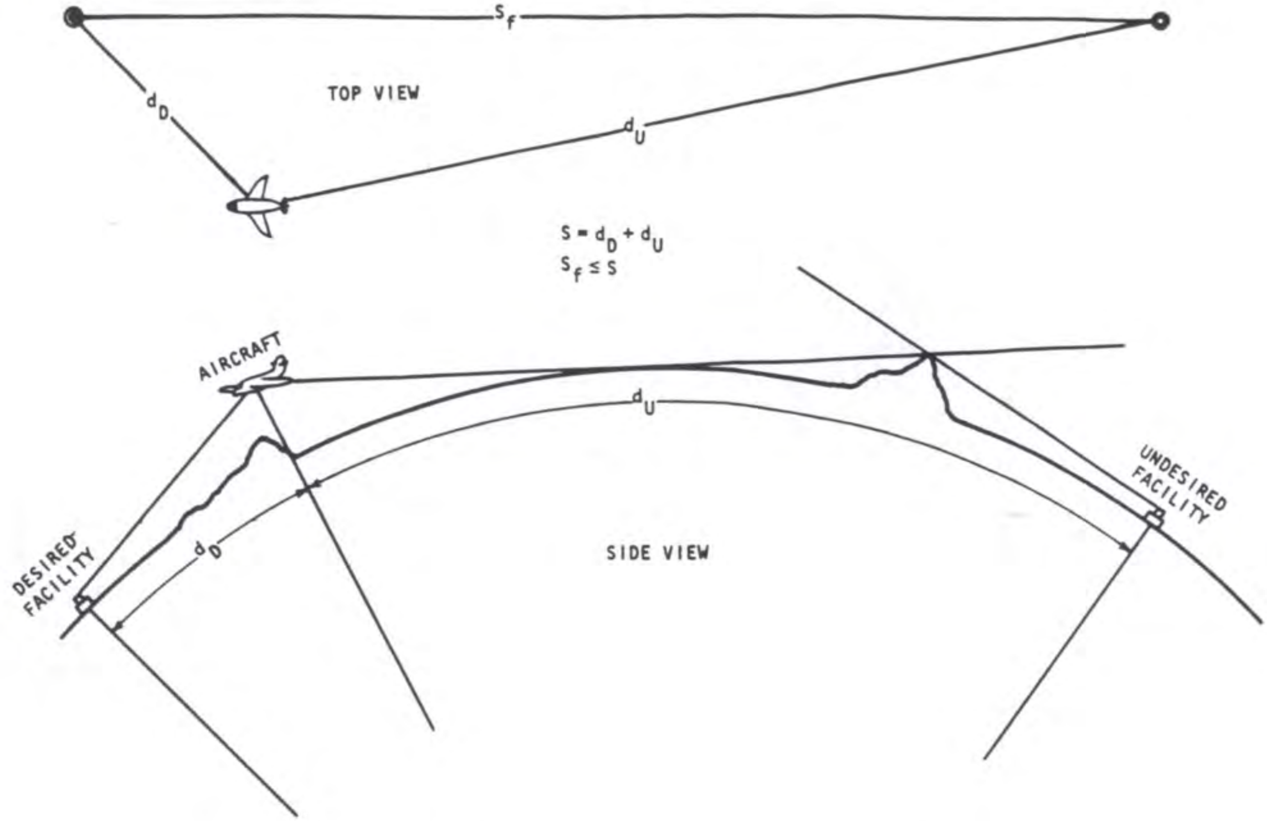

Figure 6. Sketch illustrating interference configuration.

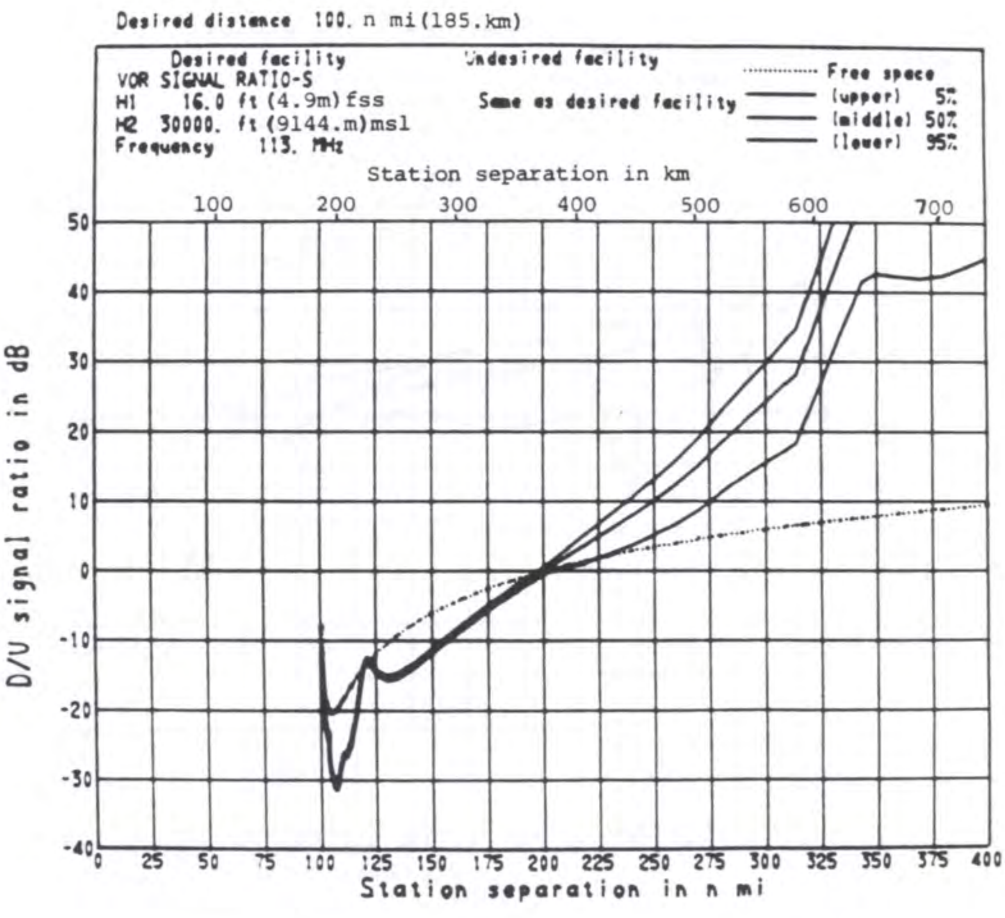

Figure 7. Plot for capability 24, SIGNAL RATIO-S.

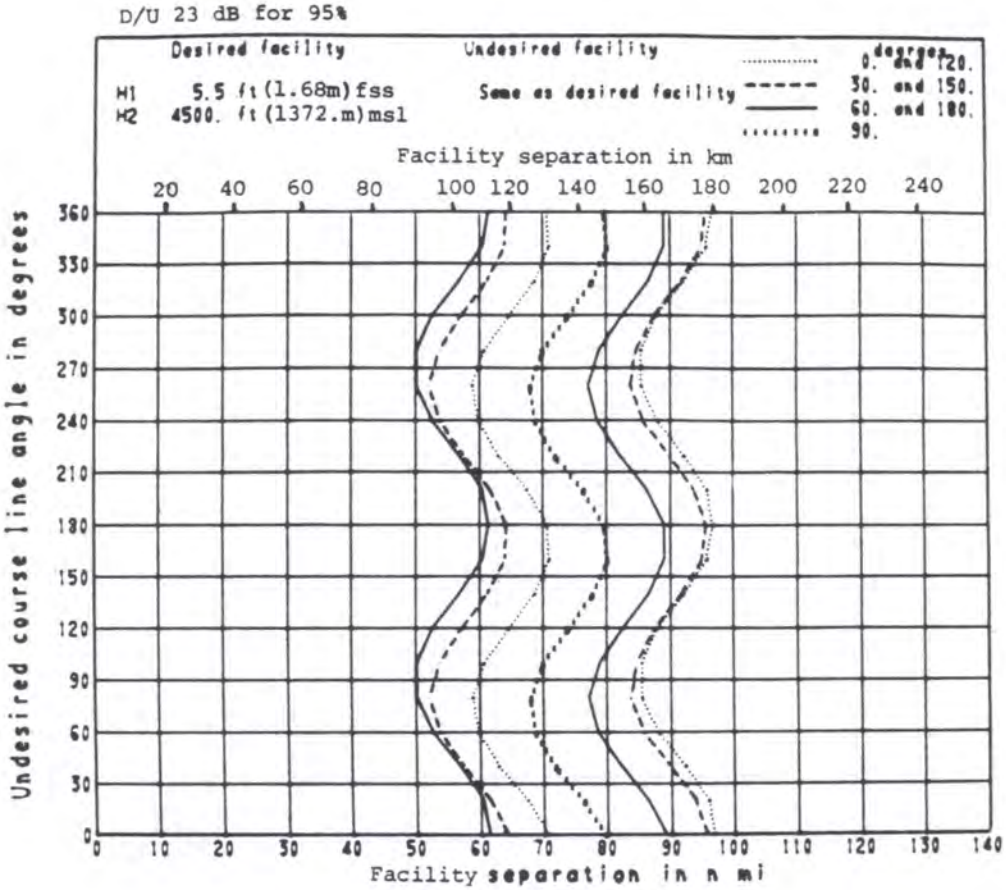

Figure 8. Plot for capability 26, ORIENTATION.

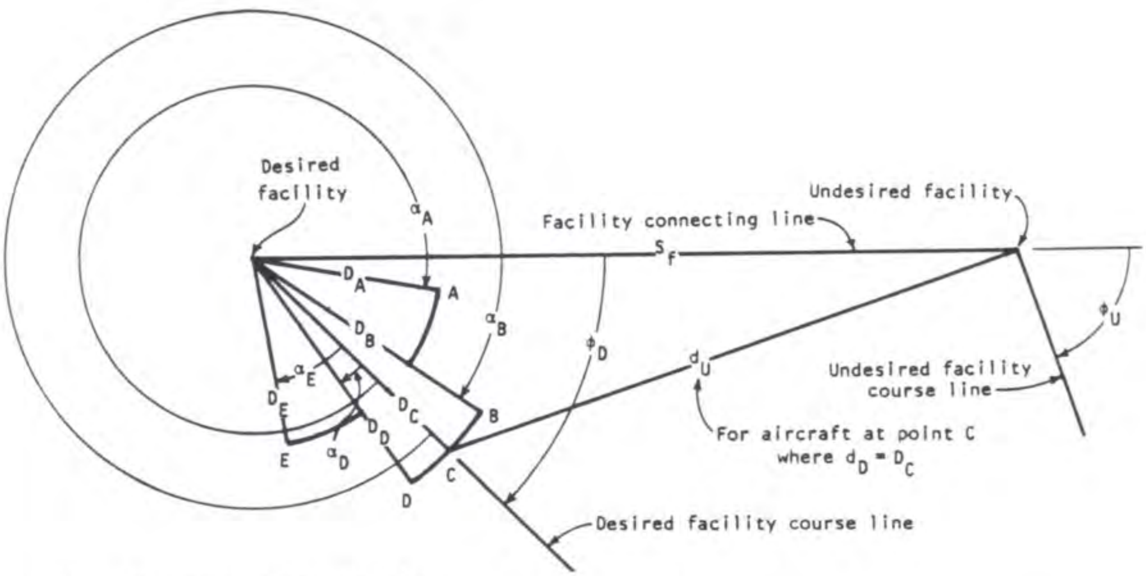

All angles are positive clockwise.

Angles to course lines, $\phi_{D,U}$, are measured from facility connecting line.

Angles to protection points, $\alpha_{A,B,C,D,E}$, are measured from the desired station course line.

Point C is along the course line so that $\alpha_C = 0$, but this is not a required condition.

Facility separation, S_f, is in general less than station separation, S, when S is calculated from $S = d_D + d_U$ where $d_{D,U}$ are facility to aircraft distances. This is illustrated for protection point C.

Figure 9. Sketch illustrating protection point geometry.

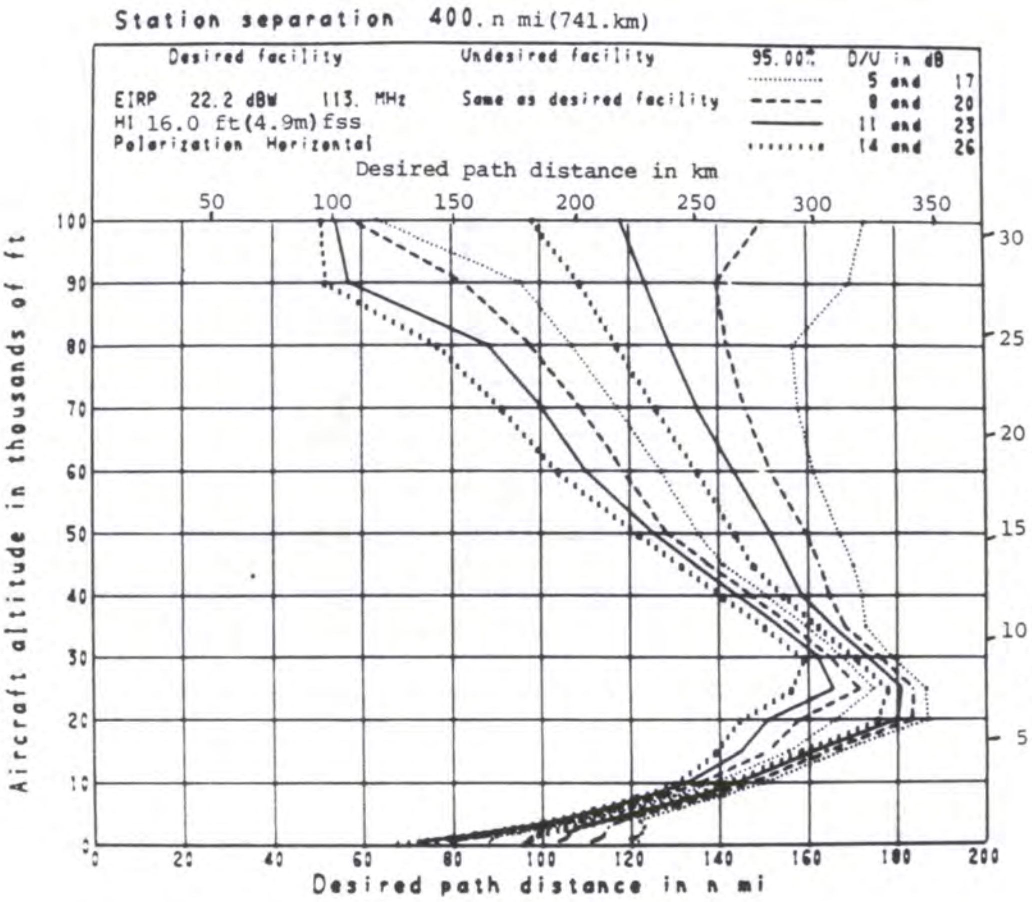

Figure 10. Plot for capability 28, SIGNAL RATIO CONTOURS.

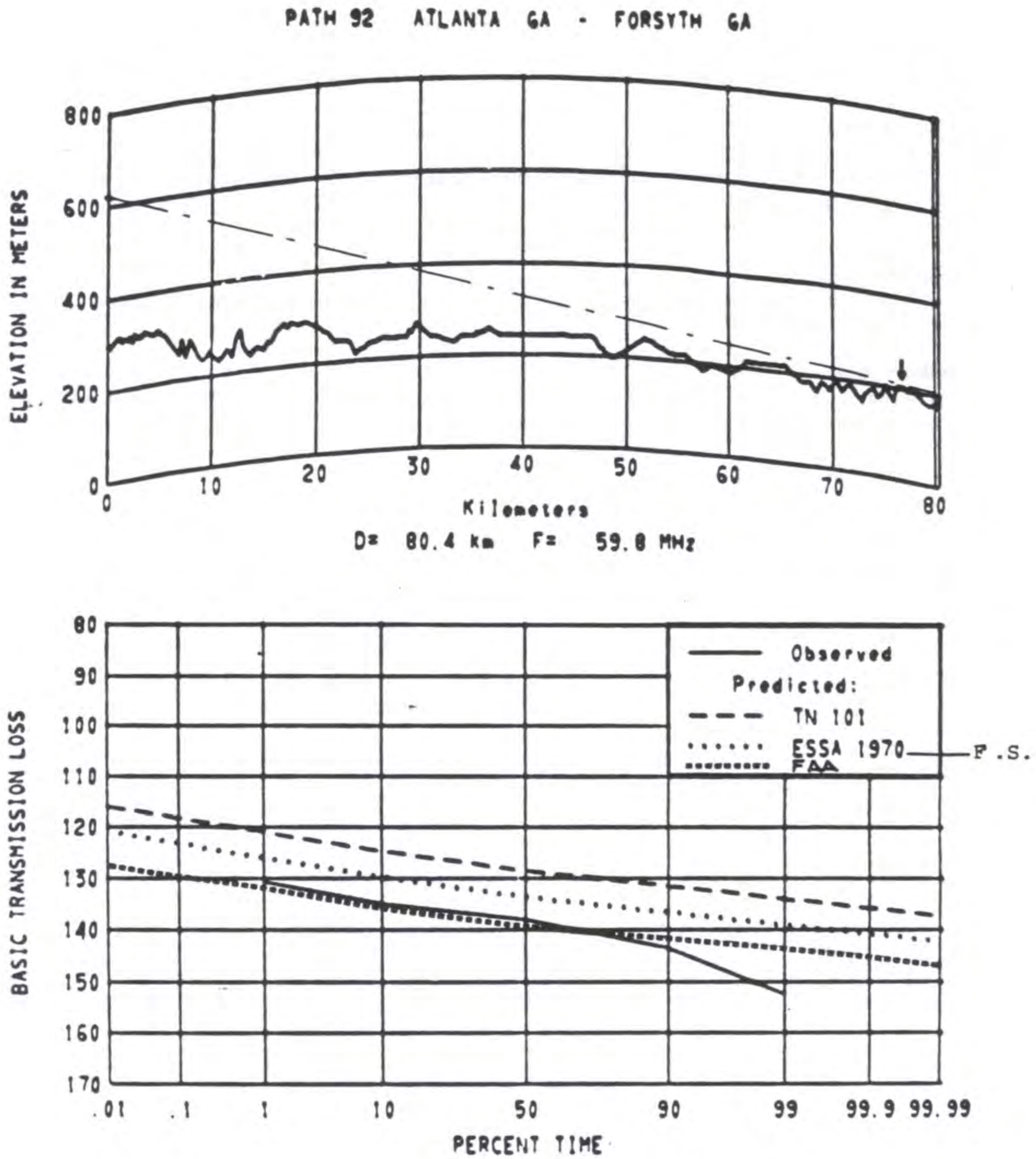

Figure 11. Profile, data and predictions for path 92.

DISCUSSION

H.Vissinga, Netherlands

Is distortion by multipath propagation included in the IF-77 model, and if not, are there plans to include it?

Author's Reply

Distortion, as such, is not predicted, and such model extensions are not currently planned. However, the time lag (Figure 2, # 4) and spectral plot (Figure 2, # 10) capabilities may be useful in distortion estimation for multipath due to a specular reflection from the earth.

J.Röttger, FRG

What is the reason why you have not included specifically the role of quasi-specular reflection at thin stratified layers in your model?

Author's Reply

While the model does not treat these reflections in a deterministic manner, their effects are accounted for in the long-term variability portion of our model (Sec. 2.3).